Structural Analysis of Historical Constructions, New Delhi 2006
P.B. Lourenço, P. Roca, C. Modena, S. Agrawal (Eds.)

AE Structural Assessment of a XVIIth Century Masonry Vault

A. Carpinteri, S. Invernizzi and G. Lacidogna
Politecnico di Torino, Department of Structural Engineering and Geotechnics. Torino, Italy

ABSTRACT: In the present paper, we describe the experimental and numerical assessment of a XVIIth century masonry vault, which was required because of the change in use of the upper floor. During the in situ load test, we recorded the Acoustic Emissions (AE) from the vault, as well as displacements of the vault and strains in the steel rods. We compare the experimental data with the numerical results obtained from finite element modeling of cracking and crushing. After validation, the model allows us to assess the ultimate load bearing capacity of the vault.

1 INTRODUCTION

The "Ospedale S.Giovanni" in Turin (Italy) is a masonry building complex initiated in 1680, under the design of the architect Amedeo di Castellamonte (Fig. 1a). The first floor of the building (realized around 1762) will soon host an important fossil collection of the Regional Museum of Natural Science. Due to this change of use, an assessment of the structural load capacity of the masonry vault beneath the first floor (Fig. 1b) is necessary, because the fossil collection will involve a sensible increase in the vault load.

To this purpose, a detailed geometrical survey of the 30m long and 10 m span barrel vault has been carried out, in order to build a fully 2D finite element model of the vault, taking into account also the presence of steel rods placed to bear part of the horizontal thrust from the vault.

The load bearing capacity of the vault has been assessed by means of an in situ loading test. The load has been applied using three water cushions, each one capable of exerting a pressure of 5500 Pa. During the loading and unloading phase, the vault deflections were recorded, as well as the increase in the steel rods tension. On the other hand, the initial stress in the steel rods had been determined from the first bending frequency during a dynamic test.

The masonry vault was also instrumented in order to record the Acoustic Emission (AE) continuously during the loading-unloading procedure. This technique was firstly used in the case of masonry-vaulted structures by Hendry and Royles (1991), and has been more recently employed by the Authors in the monitoring of several historical structures in combination with numerical simulation (Carpinteri et al. 2005).

The acoustic emission vs. time observations resemble the load vs. deflection behaviour of the vault, and appear promising in relation to the practical problem of the assessment of this structure typology where deflections are very limited due to the membrane behaviour.

The structure appears to be capable of withstanding the new destination load with the only precaution of maintaining the load as symmetric as possible (organizing the move of the collection with a correct sequence).

Finally, the nonlinear numerical simulations have been carried out to the collapse of the structure in order to provide an assessment of the safety factor of the structure.

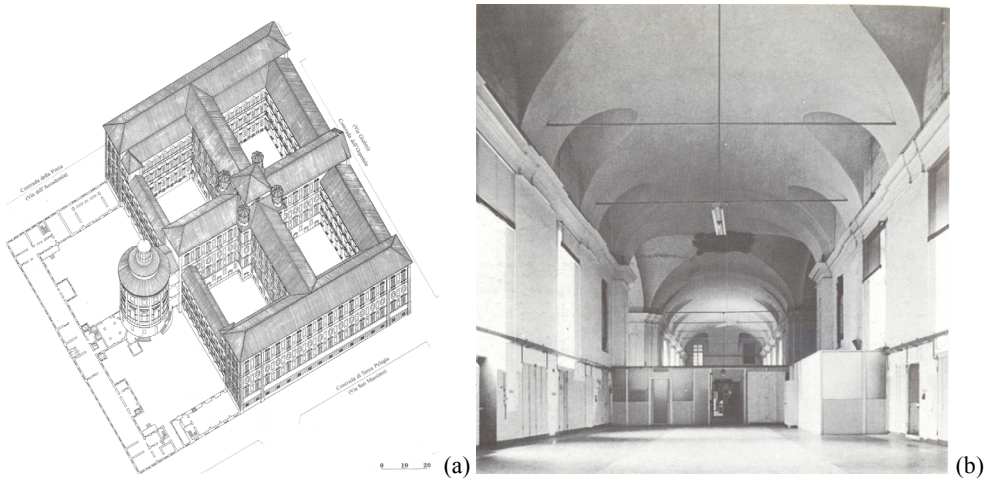

(a) (b)

Figure 1 : Aerial view of the building (a), inside picture of the vault (b).

2 GEOMETRICAL SURVEY

The geometry of the masonry vault is probably the most important factor influencing the mechanical behavior of the structure. Therefore, we started from a detailed 3D acquisition of more than 400 points, performed with an automated optical instrument (Sokkia SEF 4110R).

Fig. 2a shows a section of the building, while Fig. 2b details the position of the water cushions used for the loading test, and the measurement points where displacement and/or deformations were recorded.

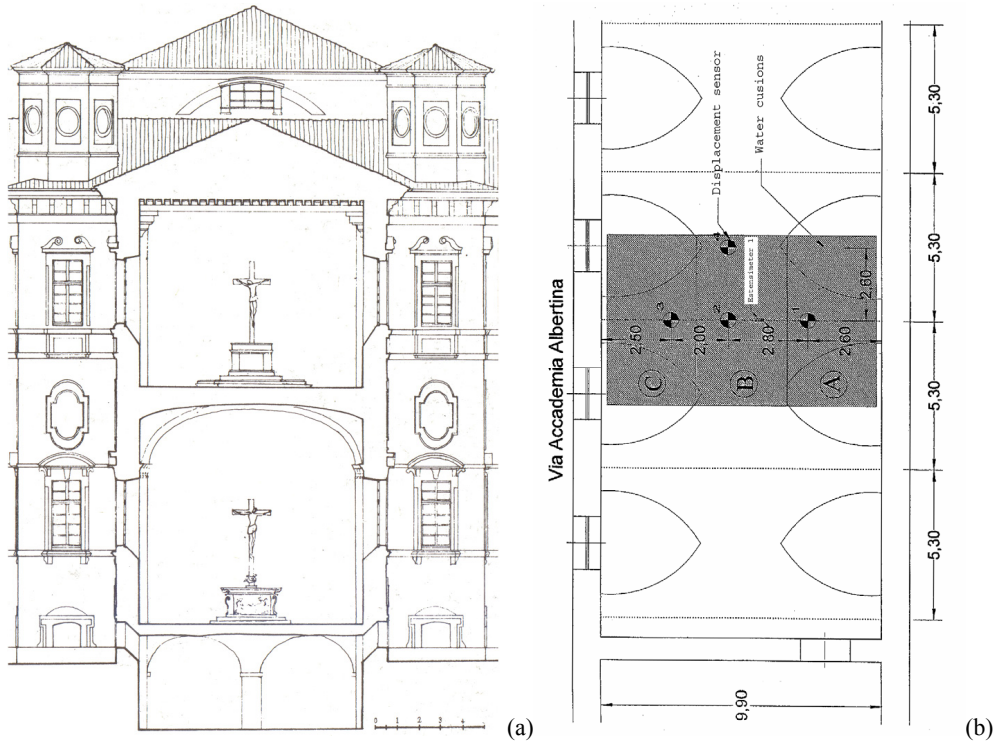

(a) (b)

Figure 2 : (a) Section of the building; (b) scheme of the barrel vault with indication of the water cushions (A, B and C) and positions of the measurement points.

3 IN SITU LOAD TEST

First, the efficiency of the steel rods against the horizontal thrust of the vault has been evaluated through a dynamical test. The first natural frequency of the rod has been recorded with a piezoelectric accelerometer (PCB model M601A02, frequency range 0.27 to 800 Hz). The normal load N, in a cable can be expressed as:

$$N = 4\frac{A\gamma l^2 f^2}{g}, \tag{1}$$

where A=13.85cm^2 is the cross section of the cable, γ=0.00768 kg/cm^2 the steel density, l=9.00 m the span, f the first natural frequency, and g the gravity acceleration. Since the measure frequency was ranging from 5.96 Hz to 7.52 Hz, the mean tensile stress in the rods was equal to 0.12 Mpa. This means that the steel rods are not acting under the effect of the only dead load.

Subsequently, an in situ load test has been performed using three water cushions to apply the load. Each of the cushions is capable of exerting a pressure of 5500 Pa. The load has been applied gradually, avoiding excessive eccentricity of the load, following the scheme shown in Fig. 3. During approximately ten hours, the load was applied and removed. During the whole period, we measured the vertical displacements of the vault (four sensors MIDORI LP50) in the points 1 to 4 shown in Fig. 2b.

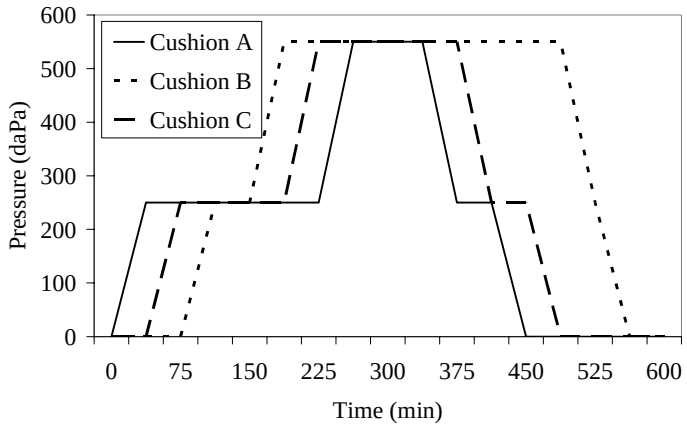

Figure 3 : diagram of the loading and unloading procedure.

Moreover, the steel rods were instrumented with extensometers (Micro-Measurements Division, type CEA-06-125UT-120) in order to measure the strains during the loading-unloading cycle. Therefore, it was straightforward to obtain the stress and normal thrust provided by the rods. Each rod starts loading as the load exerted by the cushions increases, meaning that they are well anchored to the walls. The maximum stress recorded was about 15 MPa, while no sensible permanent stresses were in the cables after that the load was removed.

Close to the measuring points 1 to 3 (Fig. 2b) also AE sensors have been used to monitor the load test.

3.1 Acoustic emission equipment and signals analysis

The cracking process taking place in some portions of the masonry vault during the loading test was monitored using the AE technique. Crack advancement, in fact, is accompanied by the emission of elastic waves, which propagate within the bulk of the material (Fig. 4a). These waves can be captured and recorded by transducers applied to the surface of the structural elements (Carpinteri et al. 2004a, b, Carpinteri and Lacidogna 2006).

The AE measurement system used by the authors consists of three piezoelectric (PZT) transducers, calibrated on inclusive frequencies between 50 and 500 kHz, and six control units. The AE sensors were placed at the intrados of the vault, close to the points where vertical displace-

ments were also acquired (Fig. 2b points 1, 2 and 3 respectively). The threshold level for the signals recorded by the equipment, fixed at 100 μV, is amplified up to 100 mV. The system does not provide for the analysis of signal frequency. The amplification gain, given the relationship dB = $20\log_{10} E_u/E_i$, where E_u/E_i is the ratio between the input and the output voltage, turns out to be 60 dB. This is the signal amplification value generally adopted in monitoring AE events in concrete (Ohtsu 1996, Shah 1994).

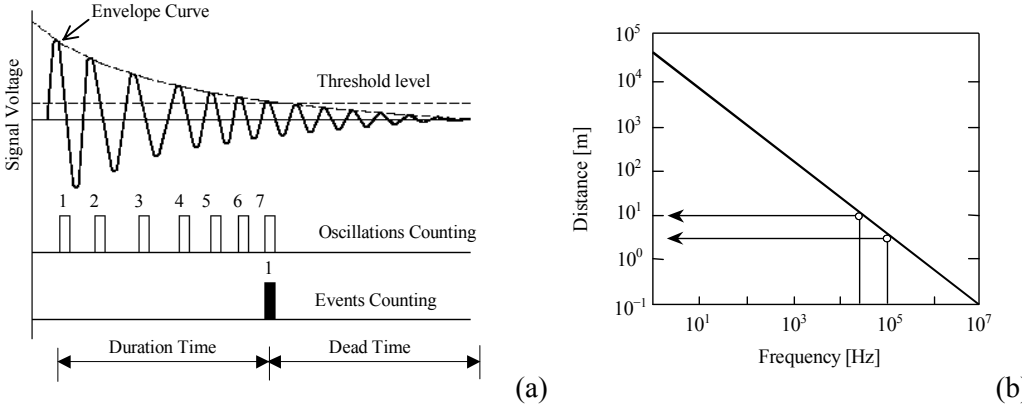

Figure 4 : (a) Signal identified by the transducer and counting methods in AE technique; (b) acoustic emission relationship between signal detection distance and signal frequency.

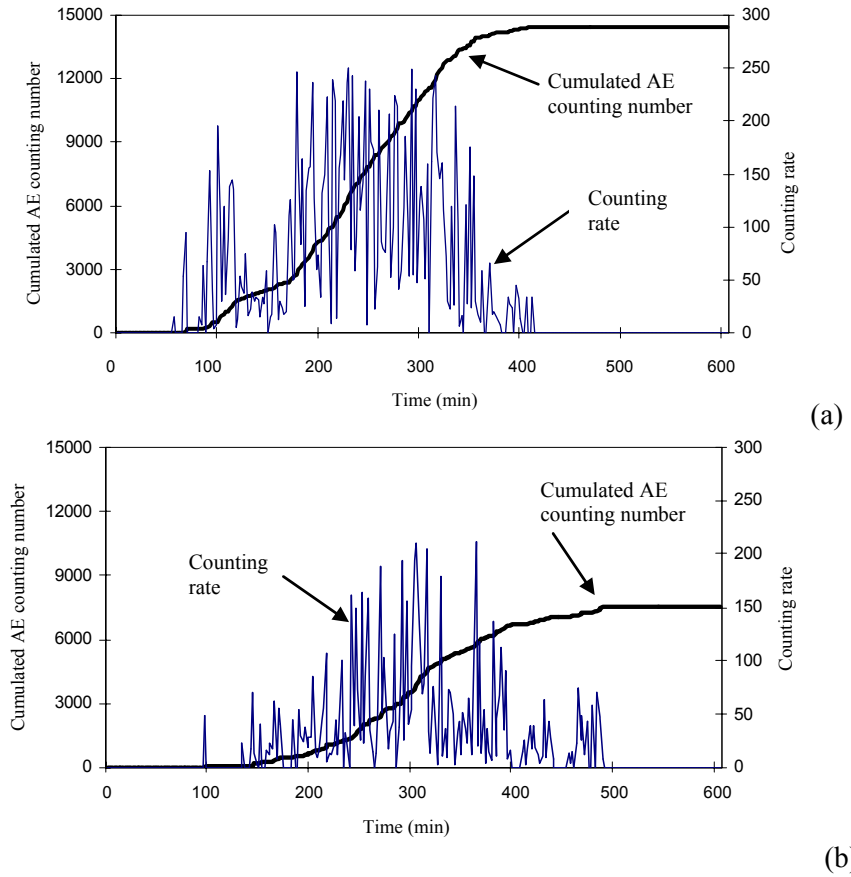

Figure 5 : (a) AE signal of the sensor in position 1; (b) and close to the vault key, sensor in position 2.

The oscillation counting limit was fixed at 255 oscillations every 120 seconds (Carpinteri and Lacidogna 2006). This procedure is referred to as Ring-Down Counting, where the number of counts is proportional to crack advancement. The exponential decay of this signal with respect to time, for a single cracking event, is shown in Fig. 4. The number of counts (N) is obtained by

determining the number of times that the signal crosses a certain threshold voltage. The crack growth rate is related to the initial magnitude of the AE elastic wave.

However, multiple events, which occur simultaneously, will also produce a large count. From the literature we know that the duration of a signal emitted during the cracking of a non-metallic material, such as concrete, is around 2000μs and that the maximum amplitude of a direct non-amplified signal is greater than 100μV. Accordingly, since attenuation phenomena can be eliminated by reducing to a few meters the distance of the transducers from the signal generation point, it can be assumed that the system of measurement is able to detect the most meaningful AE events reflecting the evolution of cracking phenomena in the masonry. Attenuation properties, in fact, depend on the frequency range: higher frequency components propagate in masonry with greater attenuation. Based on experimental results (Fig. 4b), for a measuring area at a distance of 10 m, only AE waves with frequency components lower than 100 kHz are detectable (Ohtsu 1996). In any case, utilizing the Ring-Down Counting method, and neglecting the material attenuation properties, the AE counting number (N) can be assumed proportional to the quantity of energy released in the masonry volumes during the loading process (Brindley 1973, Pollock 1973).

3.2 Detection of damage in the masonry vault

The AE sensors placed on the masonry vault indicate that some damage took place in the vault during the load test. The cumulative events and counting rate are diagrammatized in Fig. 5, respectively in proximity of the half-span and close to the abutment.

The diagrams of the sensor in position 1 indicate a higher activity with respect to the sensor in position 2. It is worth noting that AE are recorded only if the vault is loaded up to a load never reached before. Therefore, no emission takes place in the very first part, as well as in the unloading part of the diagram.

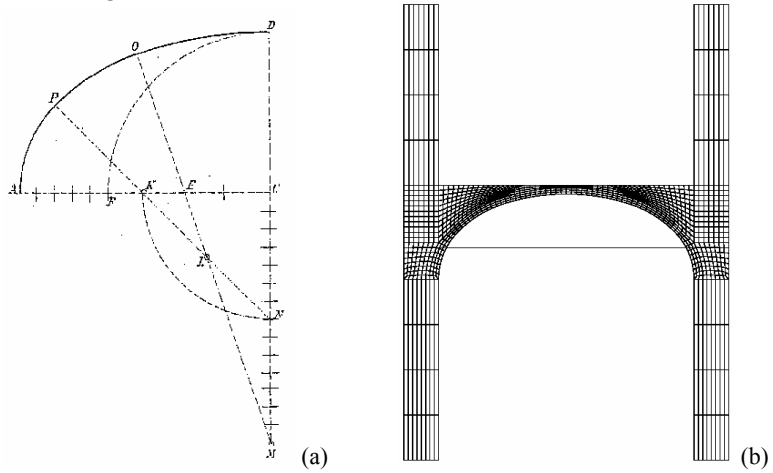

(a) (b)

Figure 6 : (a) Approximate construction of the polycyclic vault line; (b) mesh of the FEM model.

4 FEM MODEL OF CRACKING AND CRUSHING

In order to simplify the analysis, a 2D model is considered from the 3D geometry of the vault, taking into consideration a section made in correspondence of the steel rod. The continuum is discretized with eight node quadratic plane stress elements, while the steel rod is a truss element connected with nodes at the exterior sides of the walls (in order to simulate external steel bolts). The masonry walls are represented for their entire height, to account for their constrain effect. Only the lower nodes, at the basement, are pinned. The constitutive law of the masonry is assumed as perfectly plastic in compression (compressive strength equal to 3.0MPa), and with linear softening in tension (tensile strength equal to 0.3 MPa, fracture energy equal to 50 Nm).

Cracking is considered with a fixed crack smeared approach based on a total stress-strain formulation.

The Young's modulus of the masonry is equal to 2 Gpa, and the Poisson ratio is equal to 0.2, while the density is 1800 kg/m^3. The filling material above the arch is less dense (1500 kg/m^3) and more compressible (E=0.5 GPa). Moreover, it is reasonable to consider it much less strong (tensile strength equal to 0.1 MPa).

The load is applied in the model according to the experimental order. First the dead load, then, after that the truss element is activated (to account for the rod being unloaded at this stage), the external load following the scheme in Fig. 4.

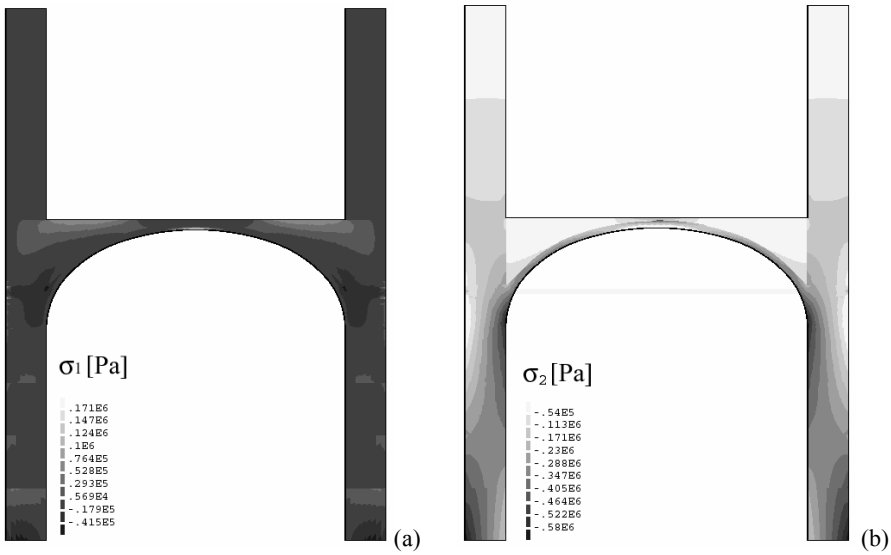

Figure 7 : (a) Structural analysis of the vault subjected to the dead load. Principal tensile stress contour; (b) principal compression stress contour, which emphasizes the shape of the thrust line.

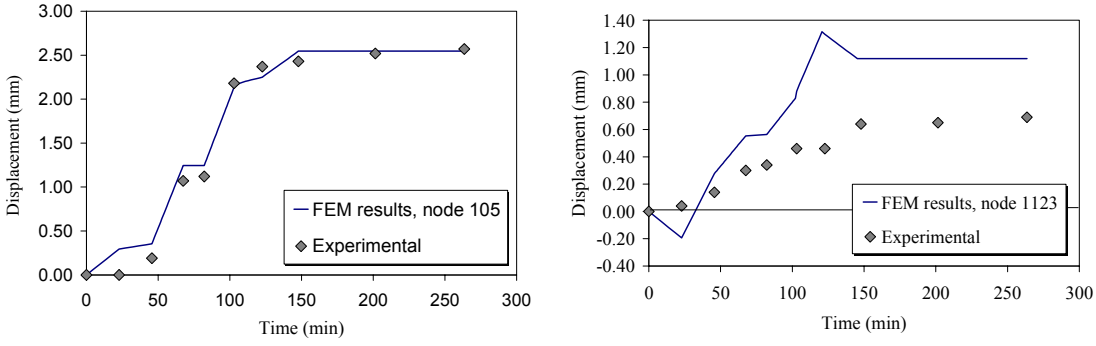

Figure 8 : (a) Time-displacement diagrams at point 2, node105, (b) and at point 1, node1123.

Three basic results validate the model. If only the dead load is considered (Fig. 7), no cracks arise in the model, which is realistic. Moreover, when the load provided by the cushion is accumulated we get a good estimate of the rod stress (16 MPa). Finally, we get a very good approximation of the time-displacement diagram under the measurement point 2 (corresponding to node 105 in the model).

The time-displacement diagram under the measurement point 1 (close to the abutment), shown in Fig. 8b, is not as good as the preceding one but still reasonably good.

The crack pattern at the end of the experimental loading procedure is shown in Fig. 9a. Very moderate cracking emerges at the intrados of the midspan. Cracks are detected only at the integration points closer to the intrados. On the other hand, more cracking takes place in the filling material above the vault. This compares well with the AE measurements that indicate higher emissions at those positions.

Finally, the numerical simulation has been prosecuted up to the final collapse of the vault. The collapse mechanism and crack pattern is shown in Fig. 9b, while Fig. 10 represents the complete load vs. displacement diagram at node 105.

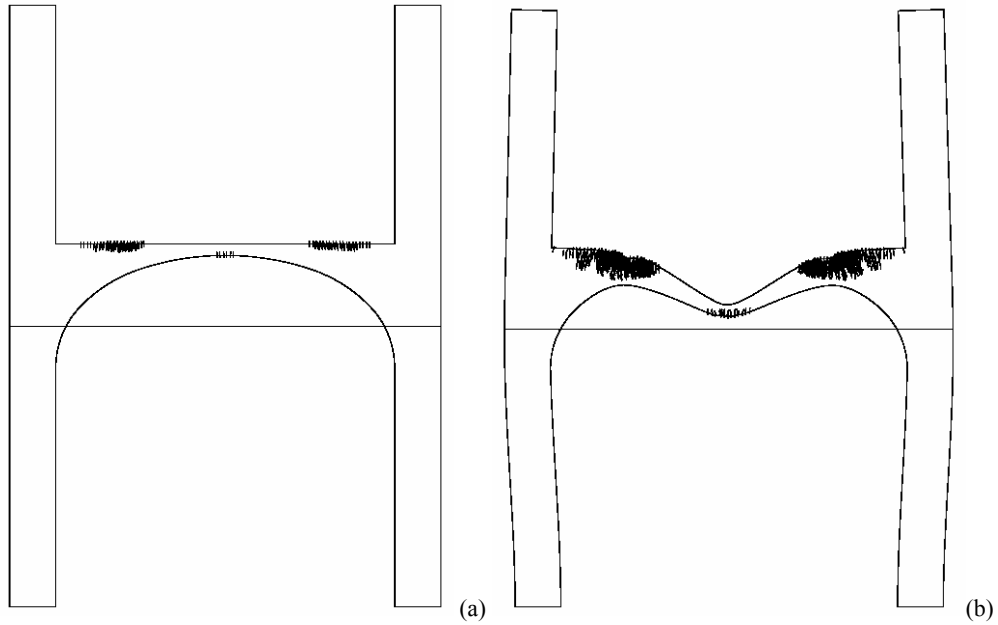

Figure 9 : (a) Crack pattern at the maximum experimental load; (b) and at the ultimate load.

It is worth noting that many convergence problems arise attempting to obtain this curve. In order to get a solution, the convergence criterion has been relaxed (energy criterion, tolerance equal to 1%). Therefore, we are fully confident of the curve only at load levels lower than approximately 1000 daPa (which corresponds to a safety factor of about 2). The final part of the plateau represents the collapse mechanism. Further analysis should be required to investigate possible more brittle behaviors.

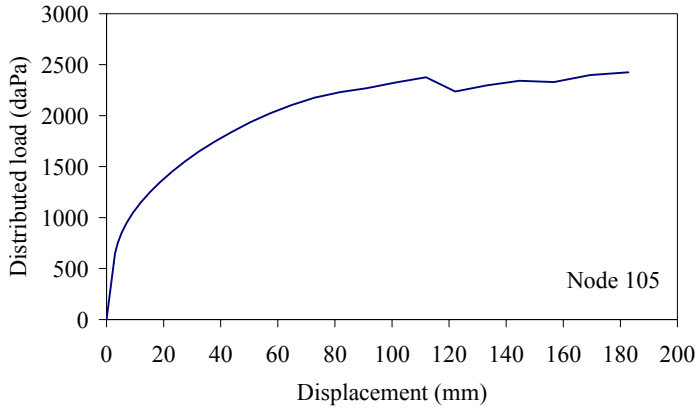

Figure 10 : Complete load vs. displacement curve (at node 105).

5 CONCLUSIONS

We presented a combined experimental and numerical study of a XVIIth century masonry vault, in order to assess the stability of the structure with respect to higher loads coming from the change in the use destination of the building.

The AE technique allowed us to detect the damage occurring both in the masonry vault and in the filling material above the vault.

The nonlinear numerical simulation of cracking confirms quite precisely the experimental results, and allows interpreting them correctly. Moreover, the numerical analysis can provide an assessment of the ultimate bearing capacity and of the final collapse mechanism.

Finally, it is possible to compare directly the cumulative AE counting distribution with the deformation of the structure (Royles and Hendry, 1991).

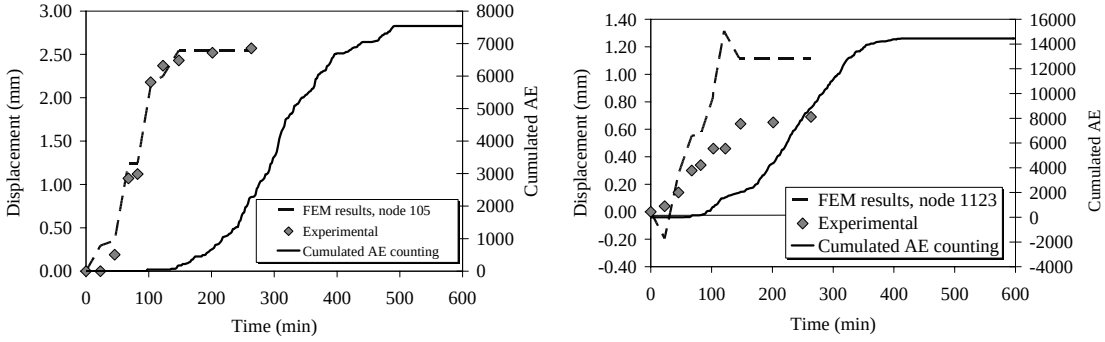

(a) (b)

Figure 11 : comparison between cumulated AE counting (right y-axis) and the experimental or FEM vertical displacements (left y-axis).

We obtained that the two diagrams (Fig. 11) resemble each other in shape quite well. Unfortunately, if the time scale is plotted without rescaling, the two curves do not match identically in the present case. Nevertheless, AE are confirmed as a useful tool to measure damage, and specifically in the case of very stiff vaulted structures.

ACKNOLEDGEMENTS

The 4EMME SERVICE S.p.a. and Ing. Flavio Camera are gratefully acknowledged for providing part of the experimental data.

REFERENCES

Brindley B.J., Holt J. and Palmer I.G. 1973. Acoustic emission-3: the use of ring-down counting. *NonDestructive Testing* 6, p. 299-306.

Carpinteri A. and Lacidogna G. 2006. Damage monitoring of an historical masonry building by the acoustic emission technique. *Materials and Structures*, in print.

Carpinteri A., Lacidogna G. and Pugno N. 2004a. A fractal approach for damage detection in concrete and masonry structures by the acoustic emission technique. *Acoustique et Techniques* 38, p.31-37.

Carpinteri A., Lacidogna G. and Pugno N. 2004b. Damage diagnosis and life-time assessment of concrete and masonry structures by an acoustic emission technique. In V. C. Li, C. K. Y. Leung, K. J. Willam & S. L. Billington, (eds), *Fracture Mechanics of Concrete and Concrete Structures*; *Proc. of the 5th Int. Conf. Vail USA*, 12-16 April 2004, 1, p. 31-40.

Carpinteri, A., Invernizzi, S., Lacidogna, G. 2005. In situ damage assessment and nonlinear modelling of an historical masonry tower. *Engineering Structures* 27(3), 387-395,

Ohtsu M. 1996. The history and development of acoustic emission in concrete engineering. *Magazine of Concrete Research* 48, p. 321-330.

Pollock A.A. 1973. Acoustic emission-2: acoustic emission amplitudes. *Non-Destructive Testing* 6, p. 264-269.

Royles, R., Hendry, A.W. 1991. Acoustic emission monitoring of masonry arch bridges. *Proc. Instn Civ. Engr., Part 2* 91, p.299-321,

Shah P., Li Z. 1994. Localization of microcracking in concrete under uniaxial tension. *ACI Materials Journal* 91, p. 372- 81.